Anatomical distribution of starch in the stemwood influences carbon dynamics and suggests storage-growth trade-offs in some tropical trees

David Herrera-Ramírez[1*], Henrik Hartmann[1], Christine Römermann[2,3], Susan Trumbore[1], Jan Muhr[1, 4], Leonardo Maracahipes-Santos[7], Paulo Brando[5,6,7], Divino Silvério[8], Huang Jianbei[1], Iris Kuhlmann[1] and Carlos A. Sierra[1]

[1]Max Planck Institute for Biogeochemistry, Hans-Knöll-Str 10, 07745 Jena

[2]Friedrich Schiller University Jena, Institute for Ecology and Evolution, Philosophenweg 16, 07743, Jena, Germany

[3]German Centre for Integrative Biodiversity Research (iDiv) Halle-Jena-Leipzig, D- 04103 Leipzig

[4]Georg August University Göttingen, Department of Bioclimatology, Büsgenweg 2, 37077 Göttingen, Germany

[5]Department of Earth System Science, University of California, Irvine, CA 92697, USA

[6]Yale School of the Environment, Yale University, New Haven, CT, United States.

[7]Instituto de Pesquisa Ambiental da Amazônia, Brasília, DF 70863-520, Brazil

[8]Department of Biology, Universidade Federal Rural da Amazônia-UFRA, Capitão Poço 68650-000, Pará, Brazil

Abstract

1. Trees balance temporal asynchrony in carbon source and sink activity by accumulating and using non-structural carbon (NSC). Previous work has demonstrated differences in the amount and distribution of NSC stored in stemwood in tropical tree species and related these patterns in NSC distribution to tree growth and mortality rates. However, we still do not know how changes in the amount and location of starch, a major component of NSC in stemwood, influence the seasonal carbon dynamics of mature trees and how this may reflect storage-growth trade-offs.
2. In this work, we hypothesized that combining two life history traits, here leaf habit (evergreen/semi-deciduous) and the anatomical distribution of starch within the stemwood (parenchyma-storage and fiber-storage), would allow us to explain differences in the seasonal interplay between carbon sources and sinks and the use and accumulation of starch in the tree stem. We expected semi-deciduous/fiber-storing species to have greater seasonal amplitudes of carbon source and sink activity, and therefore greater variation in starch content and stronger storage-growth trade-offs than evergreen/parenchyma-storing species.
3. We measured monthly increments in stem radial growth, soluble sugars, and starch every three months during 2019 in *Dacryodes microcarpa* (semi-deciduous/fiber-

storing-species), *Ocotea leucoxylon* (evergreen/parenchyma-storing-species), and *Sacoglottis guianensis* (semi-deciduous/parenchyma-storing-species).

4. We found seasonal changes in starch but not sugars in the semi-deciduous species, with greater amplitude in the fiber-storing species that also had greater storage capacity and stem respiration rates. The fiber-storing species further showed a negative relationship between starch consumption/accumulation and growth during the rainy season, suggesting a trade-off between growth and storage, with starch accumulating in some cases at the expense of growth.
5. **Synthesis:** Our results show the influence of seasonal starch storage on carbon dynamics in three species of tropical trees that differ in leaf phenology and starch storage traits. Semi-deciduous/fiber-storing species have greater temporal variation in carbon sink activities and more seasonally dynamic starch content. Since fiber-storing species tend to be slower-growing and longer-lived trees with lower mortality rates compared to parenchyma-storing species, these results may provide clues about how storage traits could influence their survival and life span.

1. Introduction

Trees assimilate CO_2 through photosynthesis to produce non-structural carbon (NSC), consisting mainly of soluble sugars, starch, and lipids. Sugars are transported to all tree organs to fuel metabolism and growth, and are locally accumulated as starch and lipids to provide energy reserves on different time scales, for example, daily, seasonal, or interannual (Chapin et al., 1990; Richardson et al., 2013). Seasonal changes in NSC content in different tree organs reflect imbalances between carbon sources (e.g., photosynthesis) and sinks (e.g., growth and respiration) (Kozlowski, 1992; Körner, 2003). Older stored carbon has been shown to fuel metabolic functions when disturbances such as defoliation or drought interrupt C supply (Hartmann and Trumbore, 2016). Information about how trees accumulate and use their NSC in key organs, such as stemwood, is needed to improve our understanding of how trees maintain their metabolism under stress.

Stemwood plays a central role in NSC dynamics and long-term storage in adult trees (Arx et al., 2017; Furze et al., 2018, 2020; Herrera-Ramírez et al., 2021). It could be the largest reservoir of NSC in trees in terms of mass due to its large volume. However, stems are also important in the transport of NSC and water between tree organs (Plavcová et al., 2016;

Furze et al., 2018). Wood is always in contact with the secondary phloem, the main tissue transporting NSC from leaves to roots and in itself an important NSC storage tissue (Rosell et al., 2021). There is constant mixing of NSC between the secondary phloem and adjacent wood tissue, allowing trees to store NSC for a long time (Furze et al., 2018, Peltier et al., 2023).

Wood anatomical traits can influence the way trees access or accumulate carbon reserves (Barbaroux and Bréda, 2002; Furze et al., 2020; Herrera-Ramírez et al., 2021). For instance, in temperate trees, traits such as vessel distribution influence not only the NSC distribution in wood but also its seasonal dynamics (Barbaroux and Bréda, 2002; Michelot et al., 2012; Furze et al., 2020). Other traits such as the formation of living fibers in stemwood (septate fibers that remain alive after maturation), or the abundance, size, and longevity of parenchyma cells, may also influence the seasonal response of NSC, overall metabolic rates, and may even be related to tree longevity or mortality rates (Arx et al., 2017; Herrera-Ramírez et al., 2021). Here, we define two starch storage traits based on the anatomical distribution of starch storages in the stemwood: 1) trees that only store starch in the parenchyma, which we refer to as parenchyma-storing species; and 2) trees that store starch in the parenchyma and living fibers, which we refer to as fiber-storing species (Herrera-Ramirez et al., 2021, Fig. S1). Herrera-Ramirez et al. (2021) demonstrated that these storage traits were related to stem growth and mortality rates for the species involved. Thus, further understanding of how this anatomical distribution of starch within the stemwood is related to the metabolism of trees and the dynamics of NSC would improve our mechanistic understanding of how tropical trees regulate carbon storage to increase competitiveness and/or survival.

On seasonal to interannual timescales, non-structural carbon storage dynamics can be controlled by physiological processes related to carbon source or sink activity under the influence of environmental conditions (Würth et al., 2005; Palacio et al., 2014; O'Brien et al.,

2015, 2020; Resco de Dios and Gessler, 2021). However, NSC storage processes can be up-regulated by increased gene expression, so reserve formation competes with other carbon sinks (Wiley and Helliker, 2012; Martínez-Vilalta, 2014; Huang et al., 2021). This may allow trees to maintain carbon stores that enable them to face future compounding perturbations (Sala et al., 2012; Dietze et al., 2014; Resco de Dios and Gessler, 2021). Storage up-regulation may be species specific (Poorter and Kitajima, 2007) and likely greater in species that store NSC for long periods of time (Blumstein et al., 2022). Tree species that rely on living fibers for NSC storage (e.g., fiber-storing species) may indicate a high priority for storage formation that would compete with other carbon sinks like growth and respiration and may be related to higher plasticity of carbon metabolism, such as higher capacity for variability of seasonal carbon fluxes (Plavcová et al., 2016; Herrera-Ramírez et al., 2021). It is possible that trees with larger plasticity in carbon storage and sink fluxes may be better adapted to stressful conditions that severely reduce photosynthesis or increase carbon demand because they may be more tolerant to a wider range of environmental conditions.

When C sources are insufficient, regulation of storage and sink activity can result in trade-offs between NSC storage and some important carbon sinks such as growth, respiration, reproduction, and production of defense compounds (Poorter and Kitajima, 2007). These trade-offs may indicate different plant survival strategies, ranging from long-lived species that may prioritize NSC storage at the expense of growth to ensure future survival, to short-lived species that invest in fast growth while storing less NSC (Wright et al., 2004; O'Brien et al., 2014; Blumstein et al., 2022). Trade-offs between NSC storage, growth, and defense have been observed in some temperate species. For example, studies have shown that the storage of NSC may be prioritized over growth under various stressful conditions such as defoliation, drought, and low atmospheric CO_2 concentrations (Anderegg et al., 2012; Hartmann et al.,

2015; Piper et al., 2015; Wiley et al., 2017; Huang et al., 2019; Piper and Paula, 2020). Allocation to defense compounds can be reduced to maintain the minimum operational storage of NSC required for survival under shade and low CO_2 (Huang et al., 2019; Huang et al., 2020). However, NSC can also be accumulated to build defenses for the future, and therefore such trade-offs may not be immediate and exhibit time lags. Thus, in many instances, trade-offs may not be clear, especially if they are measured on an annual basis.

In some cases, identifying growth-storage trade-offs can be difficult due to variability in carbon assimilation or other competing carbon sinks such as respiration and reproduction (Wiley and Helliker, 2012; Huang et al., 2019; Blumstein et al., 2022). For example, as carbon supply increases, both growth rate and NSC content may increase, masking trade-offs between the two competing sinks (Huang et al., 2019; Blumstein et al., 2022). Therefore, alternative ways to quantify these trade-offs, such as evaluating growth and storage fluxes on a seasonal basis, are needed to better understand carbon dynamics in mature trees. Furthermore, investigating the relationship between these trade-offs and tree storage traits may help us identify the influence of storage strategies on carbon dynamics in mature trees and their relationship with tree survival and recovery.

In this context, we aim to understand the influence of life history traits such as the anatomical distribution of starch storage in the stemwood (fiber-storage and parenchyma-storage, Fig. S1) and leaf habit (evergreen and semi-deciduous) on seasonal carbon dynamics of trees in response to seasonal changes in precipitation and relative humidity. For this, we propose a conceptual framework to help formulate hypotheses about the seasonal behavior of the observed carbon fluxes in four groups of trees based on the possible combinations of their life history traits (Fig. 1). Carbon fluxes were estimated based on our observations of growth, respiration, and leaf and fruit phenology collected during two years for species

143 representative of each combination of traits. We used phenological data on the percent cover
144 of mature leaves in the tree crown as a proxy for carbon acquisition. Thus, we expect
145 evergreen species to have less seasonal variations in photosynthesis rates than semi-
146 deciduous species. Although all four trait combinations are given in Figure 1, given the great
147 effort needed for seasonal analyses, we left one trait combination (evergreen/fiber-storing-
148 species) out of our sampling because previous results suggested that leaf habit did not
149 influence NSC storage, growth, or mortality in the fiber-storing species (see Herrera-Ramírez
150 et al., 2021). Thus, we focused only on three combinations of traits (evergreen/parenchyma-
151 storage, semi-deciduous/parenchyma-storage and semi-deciduous/fiber-storage) in this
152 study (Fig. 1).

153 Based on the conceptual framework (Fig. 1), we expected that: i) semi-deciduous/fiber-
154 storing species would have greater seasonal amplitude in stemwood NSC due to greater
155 seasonal variation in photosynthesis, greater demand of carbon for respiration due to a larger
156 amount of living cells, and greater seasonal variation in growth rates than the parenchyma-
157 storing species; ii) negative carbon balance during the wet season would lead to some
158 consumption of starch reserves, principally because there may be a slight decrease in
159 photosynthetic capacity (due to increased cloudiness or loss of photosynthetic tissue)
160 coincident with a large demand of carbon for growth and respiration; in which case iii) we
161 would expect to observe seasonal storage-growth trade-offs during the wet season where
162 growth would be negatively correlated with starch consumption/accumulation. In contrast,
163 we expect a smaller seasonal variation in NSC for parenchyma-storing species

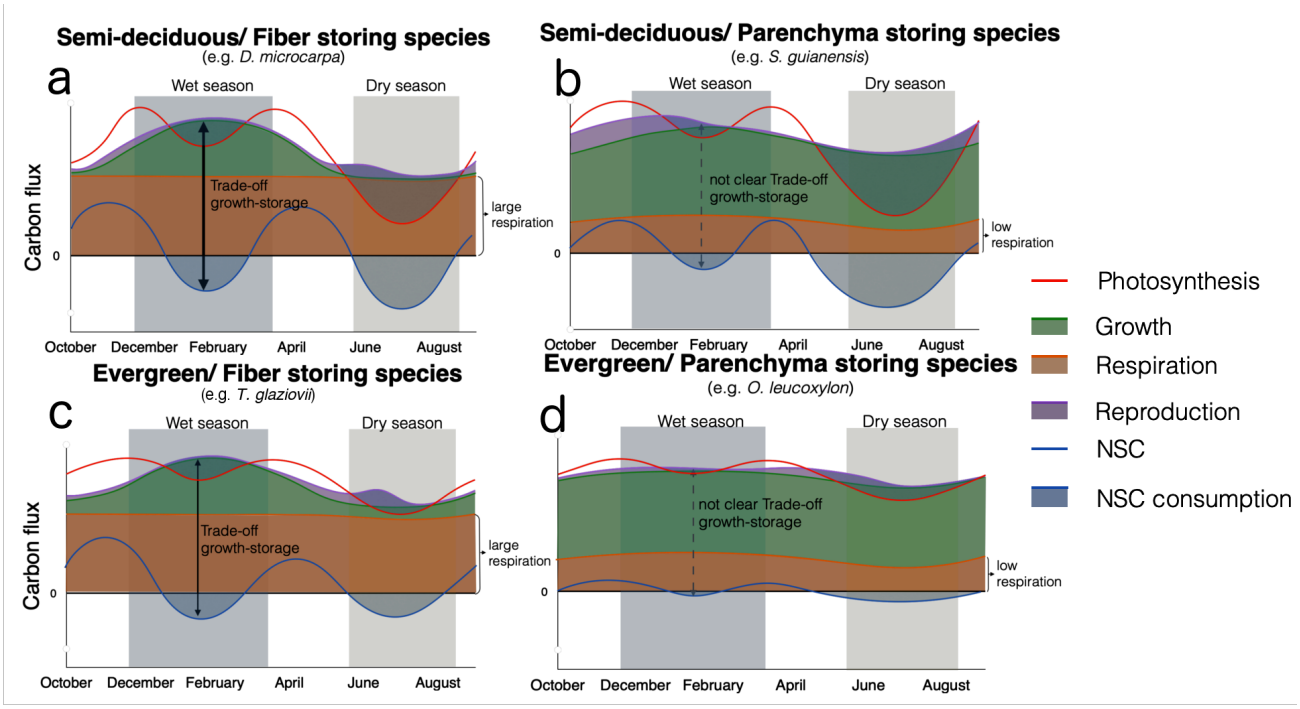

164

165 **Figure 1:** Conceptual framework illustrating temporal patterns of carbon fluxes and their
166 intraannual interactions for trees with different combinations of two life history traits: leaf
167 habit (semi-deciduous and evergreen) and anatomical distribution of starch storage in the
168 stemwood (Fiber storage and parenchyma storage) for a)semi-deciduous/fiber-storing-
169 species, b) semi-deciduous/parenchyma-storing-species, c) evergreen/fiber-storing
170 species and d) evergreen/parenchyma-storing-species). Carbon fluxes measured over a
171 year for each of these species were used to inform the seasonal dynamics of carbon
172 sources - photosynthesis (red line)- and carbon sinks - growth (green), respiration
173 (orange), and reproduction (purple) - along with their hypothesized interactions with non-
174 structural carbohydrates (NSC) storage or consumption (blue line, representing the
175 balance between previous storage, sources, and sinks). The patterns of photosynthesis and
176 reproduction were deduced from the phenological observations of mature leaves in the
177 crown of trees belonging to each of the representative species (see phenology data in Fig.
178 S3). The black horizontal solid line represents zero flux for NSC, respiration, and
179 photosynthesis. C sinks are represented as negative fluxes; The shaded colored area

beneath each carbon sink represents its contribution to the total sink flux. This conceptual (but data-informed) representation illustrates general trends. Expected seasonal trade-offs between growth and storage, manifesting as negative correlations between growth (green line) and storage (blue line), are indicated by black arrows, thicker and darker lines indicate strong (clearly observable) trade-offs, and dashed and lighter lines indicate weaker or less clear trade-offs. Under each trait combination label, we mention the representative species we measured in this study. We did not measure the representative evergreen/fiber-storing species *Trattinnikia glaziovii*, but we used previous data to inform our framework.

2. Methods

2.1. Site description

This study was conducted in a transitional forest between the closed canopy Amazon rainforest and Cerrado (savanna), located at Tanguro Ranch, Mato Grosso, Brazil. The mean annual precipitation is 1770 mm, distributed between a dry season (May to September) with less than 10 mm of precipitation per month and a wet season (October to April) with mean precipitation of 150 mm per month (Fig. 2). Relative humidity follows a similar seasonal pattern, falling below 60% from June to September and above 80% from December to February (Fig. 2). The mean temperature is 25˚C with almost no seasonal variation throughout the year (data obtained from the local station at Tanguro Ranch, operated by the Instituto de Pesquisa Ambiental da Amazônia, IPAM).

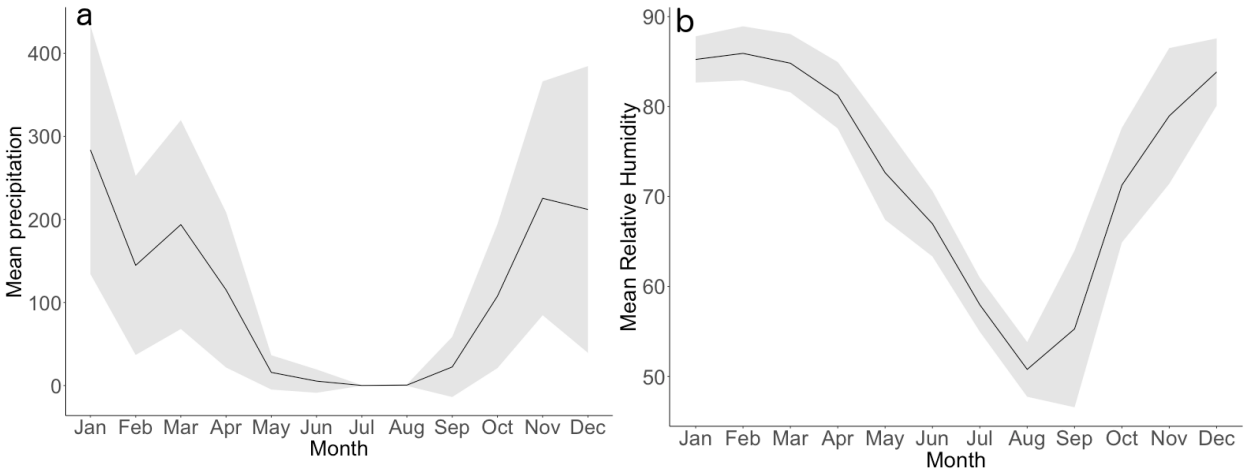

201

202

203

204 **Figure 2:** a) Mean seasonal course of monthly total precipitation (mm) and b) relative
205 humidity (%) during 2016-2020 (black lines). Gray areas correspond to the standard
206 deviation. Data were obtained from a local weather station at Tanguro Ranch (S
207 13°4'35.39'', W 52°23' 8.85'').

208 **2.2. Species description**

209 We selected three tree species previously shown to have a contrasting anatomical
210 distribution of starch storage in the stemwood: parenchyma-storing species and fiber-storing
211 species (Herrera-Ramírez et al., 2021, Fig. S1), different leaf habits (evergreen or semi-
212 deciduous), and different growth and mortality rates (Table 1). Based on inventory data,
213 these species are among the top 10 % of the most dominant species in this forest. From each
214 tree species, we chose 12 mature and healthy trees that reached the canopy with a diameter
215 at breast height (at 1.3 m, dbh) greater than 20 cm (Table 1), to ensure a representative
216 sample for each species.

Table 1: Species names and traits: wood storage strategy, growth rates, mortality rates, phenology, and sampling dates.

Species name	Growth rate (cm/year)	Mortality rate (%/year)	Anatomical distribution o starch	Leaf phenology (~% of annual leaf loss)
Ocotea leucoxylon (Sw.) Laness	0.295	5.7	Parenchyma	Evergreen (~30)
Sacoglottis guianensis Benth.	0.72	5.0	Parenchyma	Semi-deciduous (~45)
Dacryodes microcarpa Cuart.	0.078	1.6	Fiber	Semi-deciduous (~60)

*Growth rate, Mortality rates, and Leaf phenology were calculated based on inventories conducted between 2004 and 2018 and included more than 100 individuals per species.

2.3. Sampling strategy

We sampled the 36 selected trees every three months from May 2019 to February 2020, specifically in May 2019 (transition from wet to dry season), August 2019 (dry season), November 2019 (transition from dry to wet season), and February 2020 (wet season). During each field campaign, we took two wood cores (~ 5mm diameter and 20 cm long) approximately 10 cm from the previous collection point. We used one wood core to quantify the starch distribution along the radial axis from bark to pith using the histological quantification method described in Herrera-Ramírez et al. (2021). The wood cores were placed on ice immediately after collection and frozen at -18˚C within two hours to stop respiration. After freezing, they were dried at 60˚C for two days.

The second wood core was used for incubation to estimate wood respiration rates. These cores were placed in a wet tissue immediately after collection and kept away from direct

sunlight exposure. The cores were placed in the incubation chambers within two hours after collection.

2.4. NSC seasonality

We quantified soluble sugars with a High-Performance Anion Exchange Chromatography with Pulsed Amperometric Detection (HPAE-PAD) following the protocols of Landhäusser et al. (2018). We quantified starch according to the histological method proposed by Herrera-Ramirez et al. (2021). This method allows us to observe and quantify spatial patterns of starch distribution in the stemwood with high resolution and identify the cell types that were used to store starch.

To measure the concentration of sucrose, fructose, and glucose (soluble sugars), with the HPAE-PAD (Landhäusser et al., 2018), we segmented the wood core into two depth ranges: 0-2 cm and 2-4 cm. These measurements were made only for 5 individuals per species and for samples taken in January (wet season) and July 2018 (dry season). Each wood core segment was ground to a fine powder using a ball mill (Retsch MM 400, Haan, Germany) at 25 Hz for 30 seconds and dried at 60°C overnight. We weighed 50 mg of wood powder and mixed it with 1.5 ml of 80 % ethanol for 10 minutes at 90˚C to extract the soluble sugars. After cooling to room temperature, the samples were centrifuged at 13000 g for 2 minutes. The supernatant was recovered in a new vial, diluted, filtered, and then used for measuring the concentration of three specific sugars (sucrose, fructose, and glucose) by HPAE-PAD. For quality control, we used blanks, standard solutions with known concentrations of glucose, fructose, sucrose, and internal standards made of a mixture of tree leaf and branch samples as detailed in the protocol "*S3*" of Landhäusser et al. (2018). We estimated the average concentration of soluble sugars per wood core and compared them between time points. The concentration of soluble sugars was always very low (up to 2 %) for all species and we did

not find significant differences ($p>0.05$ from a Wilcoxon signed rank test) between the wet and dry season of 2018 (Fig. S2). Therefore, soluble sugars were not measured for 2019. For the species we analyzed, starch represented 70, 85, and 90 % of the stored NSC for *D. microcarpa, S. guianensis,* and *O. leucoxylon*, respectively. Therefore, we assumed that NSC dynamics are mainly represented by starch changes over time.

To quantify the starch concentration using the histological method, we took 30 μm thick slices and mounted them on a glass slide. The wood surface was covered with Lugol's iodine solution for 3 minutes to stain starch grains and then covered with a coverslip. The stained samples were photographed using an optical digital microscope with a large depth-of-field (Keyence, VHX-6000, USA) within 3 hours. Panoramic images of the sample were taken at 300x magnification.

We quantified the percentage of starch in the samples by repeatedly measuring the areal percentage of starch coverage for each 1 mm^2 area over the wood surface using the Image J software (Schneider et al., 2012). We divided the images into radial increments of 5-mm from bark to pith to measure the radial distribution of starch in the wood core. We measured starch in all 5-mm increment sections until no starch was found in the wood. While doing so, we also manually eliminated artifacts from the images that may have interfered with the quantification. After preparing the images, we ran an automatic script for identifying and quantifying starch grains in multiple 1 mm^2 regions of interest (ROI), randomly selected along the images (see the Supplementary Material Methods S2 in Herrera-Ramírez et al. (2021) for details). After identifying all starch grains in an ROI, the script calculates the percentage of the surface area covered by starch. We measured 50 ROIs in each image of 5 mm segments of the stem increment core from bark to pith. We took the average of these 50 ROI measurements as an estimate of the percentage of starch for each of the 5 mm sections of

281 the wood increment core. Measurements of the areal percentage covered by starch
282 approximate the concentration of starch per gram of dry wood, explaining 80% of the
283 variability of starch concentrations measured by the HPAE-PAD and getting close to the 1:1
284 ratio with a regression slope of 0.89 (($p<0.01$, Herrera-Ramírez et al., 2021). Finally, we
285 estimated the total starch mass of starch in the entire wood core (in grams) by integrating the
286 starch mass in each 5-mm segment along the radial path of the wood core from bark to pith.
287 The starch content (grams of starch/grams of wood) at each depth was calibrated using the
288 measured percentage of starch in the histological images. The starch mass at each wood
289 depth was estimated based on the species' wood density, segment volume, and the starch
290 content at each 5-mm of wood section.

291 We compared total starch mass and total soluble sugar concentrations in the entire wood
292 core between different sampling dates using the Wilcoxon signed-rank test with a 95%
293 confidence level, and adjusting the p values following the Holm method (Holm 1979). This
294 non-parametric test was chosen due to its robustness against potential outliers, the flexibility
295 to analyze samples coming from distinct density distributions, and its suitability for small
296 sample sizes (Hollander et al., 2013). This allowed us to identify the seasonal patterns of
297 starch mass and soluble sugars in the entire wood core of our evaluated species during 2019.

298 We estimated the seasonal amplitude of the starch concentration as the difference between
299 the maximum and minimum starch concentrations measured during 2019 across all wood
300 depths. The maximum concentration corresponds to the peak of the starch accumulation
301 period, while the minimum concentration represents the period of starch depletion. We used
302 analysis of variance (ANOVA) to evaluate differences in these starch changes between
303 different depths to determine at which wood depths the greatest changes in starch
304 concentration occurred.

We estimated the seasonal changes in the total starch mass (mg) in the entire wood core between two consecutive sampling periods as the difference between the starch mass between the two respective measurements For example, the starch change observed in the dry season was the difference in the starch mass between May 2019 and August 2019 and we denominated it May19-Aug19; Similarly, the starch change observed in the transition months from dry to wet season was the difference in starch mass between August 2019 and November 2019 (Aug19-Nov19); and the starch change observed during the wet season constituted the difference in starch mass between November 2019 and February 2020 (Nov19-Feb20). Unfortunately, due to the COVID-19 pandemic, we could not travel to the field site in May 2020 to observe the change in starch mass during the transition months from the wet to the dry season (February 2020 to May 2020) and close the year of observations.

We also estimated the relative change of the total starch mass of the entire wood core between seasons, by dividing the absolute starch mass change by the starch mass in the final month (Equation 1).

$$relative\_starch\_change = \frac{Starch_{mass}\,(t_2) - Starch_{mass}(t_1)}{Starch_{mass}(t2)} \quad \text{(Equation 1)}$$

Where t_2 is chronologically the second time point between seasons, and t_1 is the first time point.

We evaluated whether the changes in starch mass between seasons were different than zero by building 95% non-parametric confidence intervals for the mean using the adjusted bootstrap percentile (BCa) interval method (Davison and Hinkley 1997). For this purpose, we used the 'boot' package available in R (Canty and Ripley 2022). We use these intervals to graphically show differences between starch storage changes between all possible periods of

2019, within and between species. These graphical comparisons were also confirmed by a Wilcoxon rank test following the Holm method for adjusting p values (Holm 1979).

2.5. Sink activity measurements

We measured monthly stem growth with manual dendrometer bands (D1, Labcell Ltd, UK). These dendrometers were installed at breast height for each tree in July 2018, and measurements were collected monthly (by manually reading) until July 2020. We used three-month moving averages of growth rates, which we calculated to reduce the effect of water dynamics in our growth data, capturing the average intra-annual radial growth variations (Zweifel et al., 2006, 2016). From these data, we calculated the annual growth for each tree during 2019 and compared it with the mean annual starch mass and the changes in the starch mass every three months. To assess the significance of variations in monthly radial growth rates within each species, we used Wilcoxon signed-rank tests with a 95% confidence level. This test compared the growth rates between individual months. To ensure the robustness of the results, p-values were adjusted following the Holm method (Holm 1979).

To evaluate seasonal trade-offs between growth and storage, we calculated seasonally three-month cumulative growth, each corresponding to the core of the wet and dry season and the two transition periods. We estimated Pearson's correlations and linear regressions between the cumulated growth and starch mass changes for each season. The heteroscedasticity of the residuals was checked by plotting the fitted values of the model against the residuals, while the normality assumption was checked using a Q-Q plot (Fox 2015).

We measured wood respiration during the wet (May) and dry (August) seasons of 2019 by incubation of stem cores taken from each tree for 36 hours following collection. The wood cores were cut at the depth in the stem we had previously identified where starch is depleted

(6 cm for *O. leucoxylon*, 8 cm for *D. microcarpa,* and 12 cm for *S. guianensis*). The cores were then sealed in cylindrical chambers and incubated for 36 hours at ambient temperature (~25 ˚C). The CO_2 produced was collected in custom-made glass flasks. We purified the total amount of collected CO_2 after cryogenic separation on a vacuum line. We estimated the total sample mass by measuring the pressure at room temperature together with the flask volume (Muhr et al., 2018). Then we calculated the volume-specific respiration rate for each sample by dividing the total amount of collected CO_2 (in mg C) by the incubation time and wood volume of the incubated core segment. We used Wilcoxon rank tests to compare respiration between seasons and between species.

We used previous observations of leaf, flower, and fruit phenology patterns to estimate other carbon source and sink fluxes such as photosynthesis and reproduction. These observations were made for each species at this location over the last 8 years. The percentage of crown coverage of young leaves, mature leaves, flowers, and fruits has been recorded monthly from selected species. The patterns were classified into 5 categories (0, 25, 50, 75, and 100%), following the Fournier method (Fournier 1974). We used these data to estimate seasonal changes in the phenological data by fitting a smoothing spline model to the monthly data (Fig. S3). We used these phenological data to give an idea of the contribution of flowering and fruiting to the seasonal carbon sink fluxes, but we did not measure the amount of carbon allocated to these fluxes for individual trees or species. Then in general we assume a higher flux of carbon to reproduction whenever there is more presence of fruiting and flowering. We report these data in Fig. S3.

2.6. Data analysis software

All statistical analyzes and calculations were performed using the software R (R core team 2023). All graphs and figures were generated using the software R and Gimp (The GIMP development team 2019).

3. Results

3.1. Seasonality of starch mass, growth, and respiration

Quantifying starch concentrations every 5 mm of wood along the radial axis from bark to pith allowed us to estimate with high precision the radial profile of starch concentration across the sampled wood cores (Fig. 3). Starch concentrations decreased radially across the sapwood from bark to pith for all species at all sampling dates (Fig. 3). Notably, the largest differences in starch concentration between sampling dates were greater in the first 20 mm of wood for *D. microcarpa* and *O. leucoxylon,* and in the first 60 mm of wood for *S. guianensis* (Fig.3, Fig. S6, p.adj<0.05), as compared to the inner regions where starch concentrations were very low overall.

We used these radial profiles of concentrations to estimate the starch mass in the entire wood core for each tree at each time point (Fig. 4). We found significant differences in the total starch mass of the entire wood core between the sampling dates for the semi-deciduous/fiber-storing species *D. microcarpa* (p=0.01, Fig. 4a) and marginally significant differences for the semi-deciduous/parenchyma-storing species *S. guianensis* (p = 0.059, Fig. 4c), while the evergreen/parenchyma-storing species *O. leucoxylon* showed no significant differences in starch mass in the stemwood during 2019 (p>0.1, Fig. 4b). Changes in total starch mass in the entire wood core between sampling dates were greater for the fiber-storing species *D. microcarpa* than for the parenchyma-storing species *S. guianensis* and *O. leucoxylon* (*Fig. 5*). *D. microcarpa* trees significantly reduced starch mass during the dry

period May19-Aug19 by about -0.75% (*ci*: -1.15, -0.37, Fig. 5a, Fig S4). with respect to starch mass in August 2019, while *S. guianensis* had significant gains in starch mass during the period May19-Feb20 by about 0.30% (*ci*: 0.06, 0.53, Fig. 5c, Fig. S4) with respect to the starch mass in February 2020. *O. leucoxylon* reduced the starch mass during the wet period Nov19-Feb20 by about -0.30% (*ci:* -0.05, -0.63, Fig.5b, Fig. S4) with respect to the starch mass in February 2020.

Seasonality in monthly growth rates during 2019 was only significant for the semi-deciduous/fiber-storing species *D. microcarpa (p < 0.05, Fig. 6a)*. These trees grew slower during the dry season and faster during the wet season. The two parenchyma-storing species did not show a clear seasonal pattern ($p > 0.1$, for all comparisons between all months), although a slight decrease in growth rates during the dry season can be noticed for both *O. leucoxylon* and *S. guianensis* in Figs. 6b and 6c, respectively.

Wood respiration was higher in the semi-deciduous/fiber-storing species *D. microcarpa* than in the two parenchyma-storing species *S. guianensis* and *O. leucoxylon* (*p < 0.01, Fig. 7*). However, within-species differences between the 2019 wet and dry seasons were not statistically significant for any of the species (p > 0.1, Fig. 7).

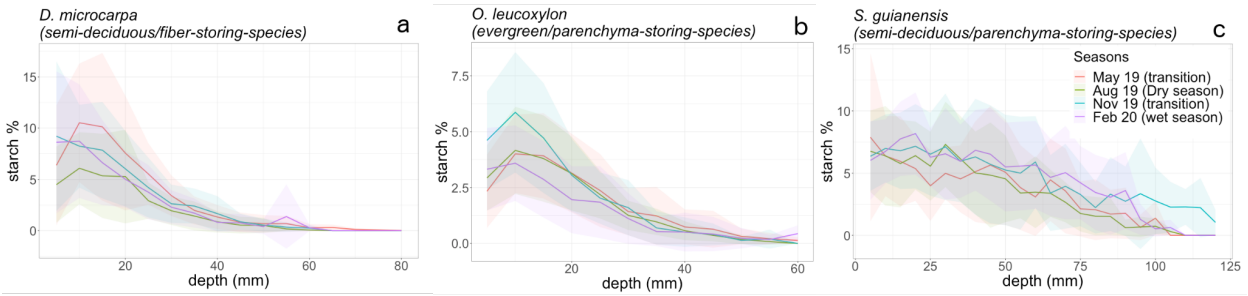

Figure 3: Radial distribution of the mean starch concentrations in the stemwood measured from bark to pith across four different months during 2019. This figure shows the average

starch concentrations, measured every 5-mm interval from bark to pith, across wood cores sampled from adult trees for a) *D. microcarpa*, b) *O. leucoxylon,* and c) *S. guianensis*. We sampled 12 mature trees from each species. Wood cores were sampled during four distinct months in the year 2019, with each month corresponding to a particular seasonal state of precipitation, as indicated in the legend. Starch concentrations were measured along the entire length of the wood cores until reaching a point where starch levels were indistinguishable from zero. The shadowed areas in different colors represent the standard variation around the mean starch concentrations for each of the measured months.

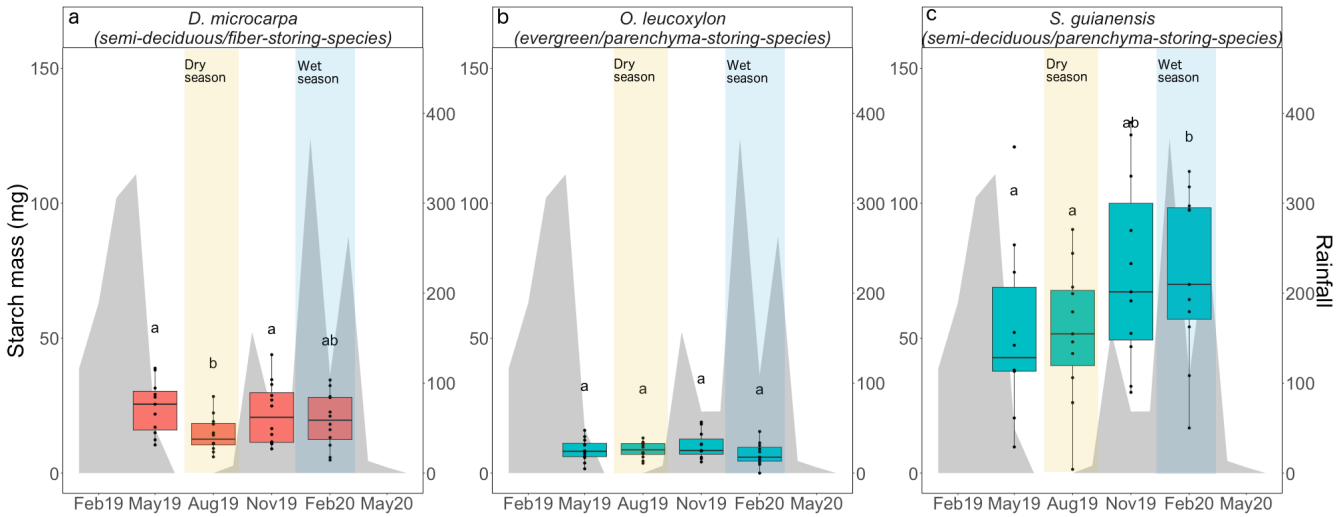

Figure 4: Distribution of the wood core starch mass at each time point of measurements for a) *D. microcarpa*, b) *O. leucoxylon,* and c) *S. guianensis*. Starch mass data was obtained from repetitive measurements in wood cores from 12 trees per species across four months of the year 2019. The box-plots show the median and quartile ranges for each group, with individual measurements represented as black dots. These values correspond to the y-axis. Statistical comparisons between different temporal measurements for each species were done using a Wilcoxon signed-rank test. Significant differences between groups at a 90% confidence level are indicated by distinct letters placed above the respective box-plots.

Each panel is labeled with the species name and its specific trait combination. blue box-plots represent parenchyma-storing species, while red box-plots represent the fiber-storing species. The gray-shaded areas behind the box-plots correspond to the monthly precipitation data for the year 2019, with values provided on the right-hand y-axis. We highlighted the dry season with a yellow shading and label, while the wet season is marked with a blue shading and label.

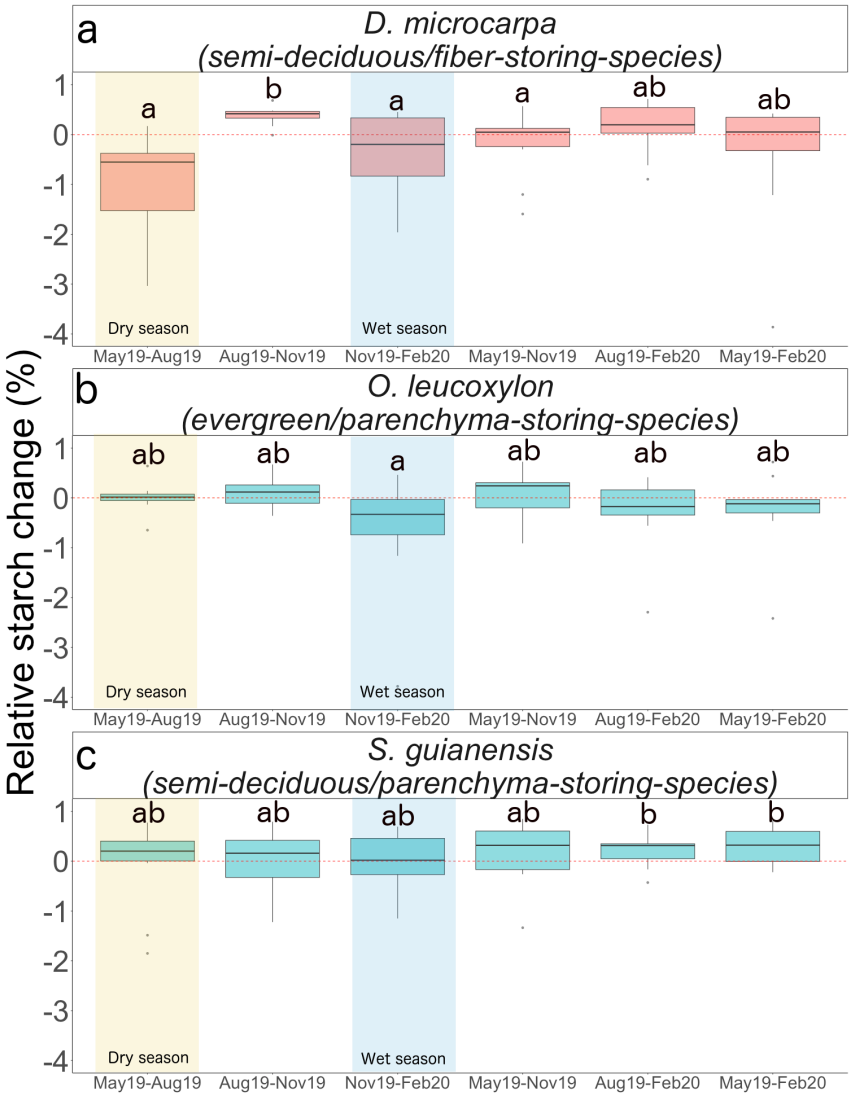

Figure 5: Relative starch changes with respect to the starch content in the final month of the evaluated period for a) *D. microcarpa*, b) *O. leucoxylon,* and c) *S. guianensis*. These relative changes were computed using Equation 1, providing a relative measure of the increase of

443 decrease in starch mass within a given time frame. We estimated these changes for all
444 possible permutations of months, keeping their temporal order. The x-axis describes the
445 evaluated periods, first denoting the initial month and then the final month. Box-plots
446 indicate the data distribution derived from measurements of 12 trees per species per time
447 point. Statistical comparisons between groups with a 95% confidence level were evaluated
448 using nonparametric confidence intervals obtained from bootstrapping methods (see Fig. S4).
449 Here, significant statistical differences occurred when the confidence intervals did not
450 overlap, denoted by distinct letters. Red box-plot represent fiber-storing species and blue
451 box-plots represent parenchyma-storing species. The wet season is highlighted with a shaded
452 blue area, while the dry season is highlighted with a shaded yellow area.

453

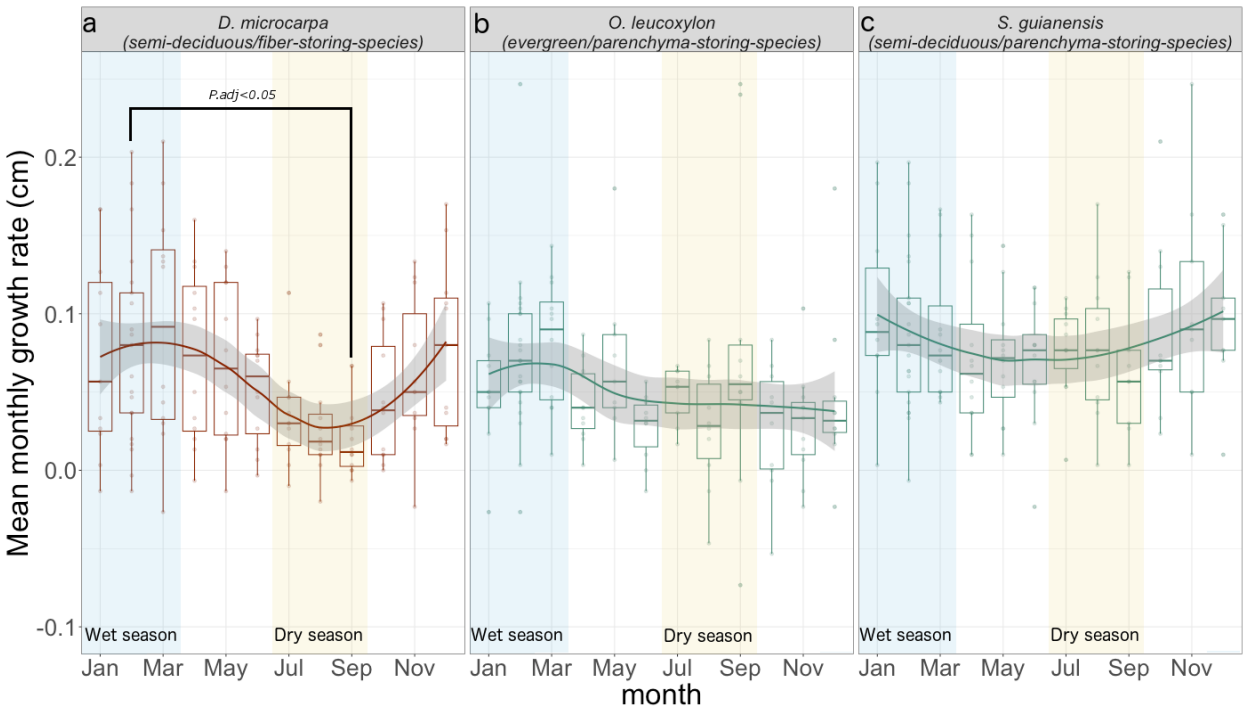

454

455 **Figure 6:** Seasonal course of growth rates for a) *D. microcarpa*, b) *O. leucoxylon*, and c) *S.*
456 *guianensis*. The figure shows the mean monthly growth rates, derived from measurements
457 of 12 trees per species throughout the year 2019. The distribution of data can be observed

in the box-plots, while the seasonal trend is shown by a smooth colored solid line across the data groups. The gray shaded areas correspond to the 95% confidence interval of the smooth line. The wet season is indicated by blue shading, and the dry season is indicated by orange shading. Comparisons between monthly growth rates within each species were statistically assessed using a Wilcoxon signed-rank test, with P values adjusted following the Holm method (Holm 1979). We only found significant differences between growth rates in February 2019 and September 2019 for *D. microcarpa* (p.adj=0.032), and this is indicated in the figure by a solid black line that connects the compared months and depicts the p-value. Each panel is labeled with the name of the species and its specific combination of traits. Red box-plots correspond to the fiber-storing species, while blue box-plots correspond to the parenchyma-storing species.

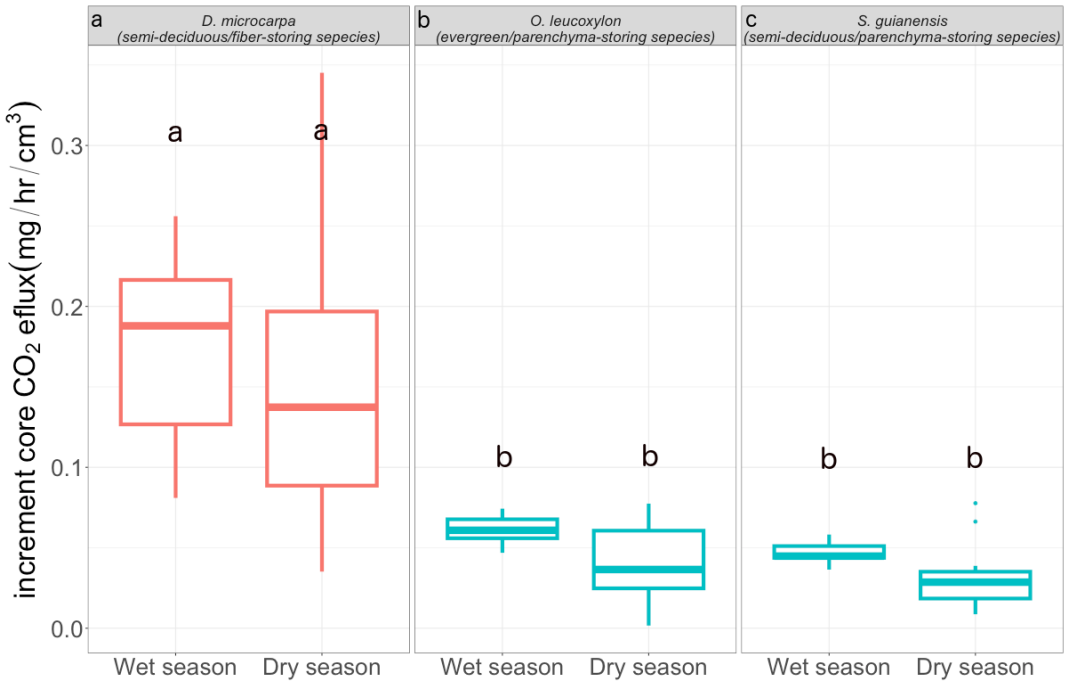

Figure 7: Seasonal variation of stemwood respiration for the evaluated species. The figures present wood respiration rates per unit of wood volume, measured in 12 trees per species during both the wet and dry seasons of 2019. The distribution of the data is shown

by box-plots. Statistical comparisons of wood respiration rates between seasons and species were evaluated using the Wilcoxon ranked test. Significant differences at the 95% confidence level are denoted by distinct letters. Each panel is labeled with the species name and its specific trait combination. The red box-plots represent the fiber-storing species, whereas the blue box-plots represent the parenchyma-storing species.

3.3. Accumulation and consumption of starch

We observed a strong significant starch consumption during the dry season (May19-Aug19) only for the fiber-storing species *D. microcarpa* (Fig. 5a, Fig. S4). The parenchyma-storing species (*S. guianensis* and *O. leucoxylon*) did not show significant starch consumption during the dry season (Fig. 5b, Fig. 5c, Fig. S4). Nevertheless, our data suggest that *S. guianensis* may consume starch during the transition months between the wet and the dry season from February to May, since the total starch mass appears to be lower in May than in February (Fig. 4c), but unfortunately, we did not measure this period in 2020.

We observed a marginally significant consumption of starch during the wet season (Nov19-Feb2020) for the fiber-storing species *D. microcarpa* (Fig. 5a and Fig. S4) and a significant consumption for the evergreen/parenchyma-storing species *O. leucoxylon* (Fig. 5b and Fig. S4).

Starch accumulation was observed during the transition from dry to wet season (Aug19-Nov20) in the semi-deciduous/fiber-storing species trees (*D. microcarpa*) (Fig. 5a). The semi-deciduous/parenchyma-storing species (*S. guianensis*) accumulated starch from May 2019 to February 2020 (Fig. 5c and Fig. S4). We did not detect a significant accumulation of starch for the evergreen/parenchyma-storing species *O. leucoxylon* ($p<0.05$, Fig. 5b).

3.4 Seasonal storage-growth trade-offs in stemwood

During the wet season (Nov19-Feb20), we observed a negative correlation between the cumulative three months of growth (Nov19-Feb20) and the changes in starch mass during the same period, for the semi-deciduous/fiber-storing species *D. microcarpa* (p = 0.05, r^2 = 0.36, Fig. 8c). During this period, some trees consumed starch while growing rapidly, and some other individuals accumulated starch instead and had lower growth rates (Fig. 8c). For this species, most individuals had high starch consumption during the dry season, but this was not associated with growth (Fig. 8a).

For the parenchyma-storing species *O. leucoxylon* and *S. guianensis*, the storage-growth trade-off was less clear or absent. We did not observe a significant correlation when comparing concurrent growth and starch change during each season ($p>0.05$). However, we found significant correlations when considering a three-month lag between growth and starch change for these species (Fig. 8, see only *O. leucoxylon* and *S. guianensis*). For example, we observed a negative correlation between the starch mass change during the transition months from dry to wet season (from August 2019 to November 2019, Aug19-Nov19) and the three months of cumulative growth in the wet season (from November 2019 to February 2020, Nov19-Feb20), for *O. leucoxylon* (p=0.03, r^2=0.41, Fig. 8e). This trend was also observed for *S. guianensis*, but it was not significant (p=0.1, r^2=0.38, Fig. 8h).

We observed that starch mass in the whole wood core was related to annual stem growth, but there were differences between storage strategies. The storage-growth trade-off trend between the starch mass in February 2020 and the annual growth calculated from February 2019 to February 2020 was still distinguishable for the fiber-storing species *D. microcarpa*, although not significant (p=0.11, r^2=0.31, Fig. S5d). The semi-deciduous/parenchyma-storing species (*S. guianensis*) showed a positive correlation between annual growth and starch mass

520 in the dry season (August 2019, *p=0.003,* r^2= 0.79, Fig. S5j), and also a positive correlation
521 between annual growth and starch mass in the wet season, although weaker (February
522 2020,p=0.05, r^2=0.51, Fig. S5l). The evergreen/parenchyma-storing species (*O. leucoxylon*)
523 showed a marginal positive relationship between starch mass in May 2019 (transition
524 between wet and dry seasons) and annual stem growth (*p*=0.088, r^2=0.4, Fig. S5e).

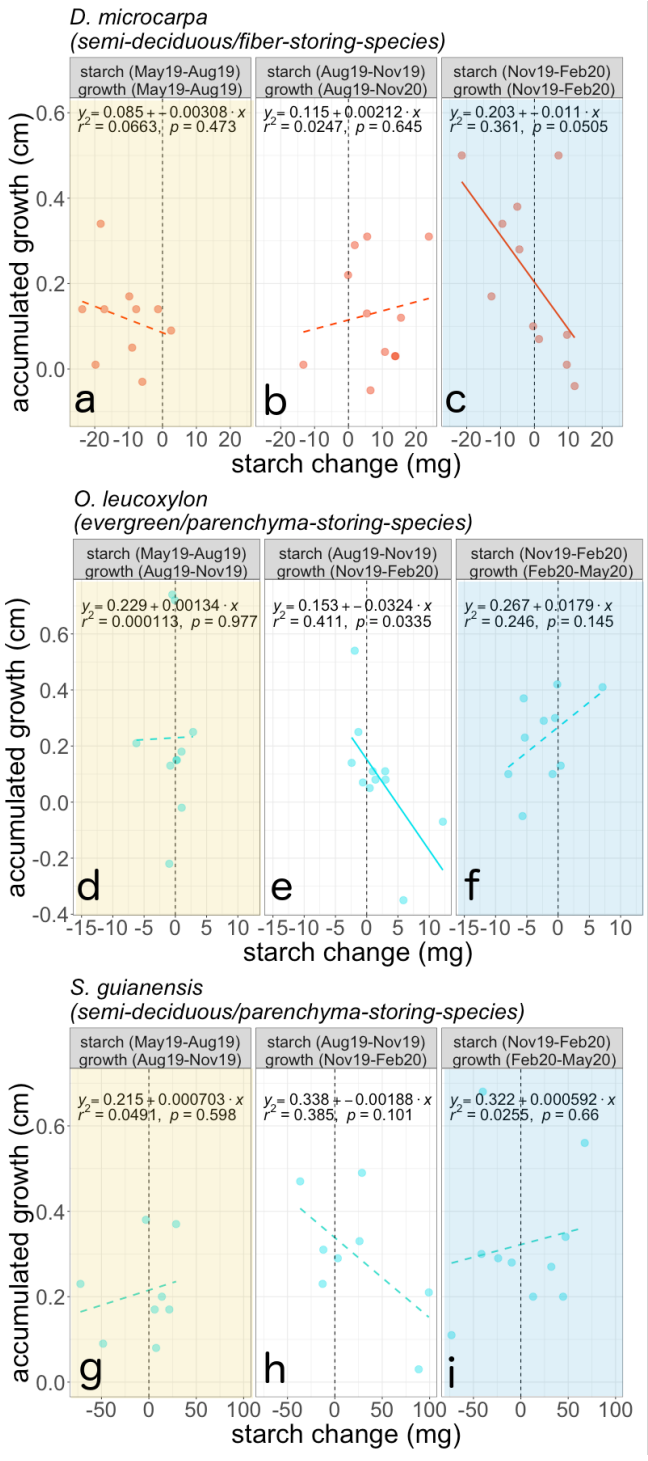

Figure 8: Relationship between changes in starch mass and the cumulative three-month growth in 2019 for the species studied. For the fiber-storing species (red

lines and dots), growth and starch changes are evaluated over the same months. Conversely, For the two parenchyma-storing species (blue lines and dots), no significant correlations were observed between growth and starch changes during the same months. Instead, starch storage shifts are correlated with growth in the following 3 months. The specific periods of comparison for starch change and growth are indicated in each panel's title. Solid lines denote significant correlations, while dashed lines represent non-significant correlations. The vertical dotted line marks the 0 in the starch change axis. Shaded yellow areas indicate the dry season, and shaded blue areas indicate the wet season. Species names and their specific combination of traits appear over the three respective sub-panels, and each sub-panel is labeled with distinct consecutive letters from a to i.

4. Discussion

Our results relate differences in carbon dynamics in mature trees to life history traits such as the anatomical distribution of starch in the stemwood and leaf habit, which we summarized in our conceptual framework (Fig. 1). Evergreen trees should not exhibit large seasonal differences in carbon acquisition, while the semi-deciduous trees studied here shed between 50 and 70% of their leaves during the dry season (May-August) and then invest carbon in new leaves (Fig. S3). Eddy covariance data from this forest indicate an overall decrease in canopy photosynthesis during the dry season (Brando et al., 2019). During the wet season (November-February), a slight reduction in the percentage of mature leaves may also indicate a slight reduction in photosynthesis (Fig. S3, Fig. 1).

The slow-growing semi-deciduous/fiber-storing species (*Dacryodes microcarpa*) showed seasonality in radial growth but not in wood respiration. This species had the largest starch consumption during the dry season, when carbon availability was low and radial growth was

almost absent, and low overall consumption during the wet season, when carbon availability and growth were higher (Fig. 5, Fig. 6). As expected, we observed a strong negative correlation between growth and starch storage change in this species during the wet season, with starch consumption when trees grew rapidly, and starch accumulation when radial growth was low (Fig 1, Fig. 8c).

The two parenchyma-storing species partially agreed with our hypothesis presented in our conceptual figure. Neither showed marked seasonality in radial growth or wood respiration. Starch mass was marginally seasonal in the semi-deciduous/parenchyma-storing species (*Sacoglottis guianensis*), with starch accumulation towards the wet season from November to February. Although we did not detect significant starch consumption during the wet or dry season, lower starch mass values in May and August 2019 suggest that these trees consume starch during the dry season. For the evergreen/parenchyma-storing species (*Ocotea leucoxylon*), we did not observe seasonality in the total starch mass, but we did detect significant starch consumption during the wet season (Fig. 5, Fig. S4). For these parenchyma-storing species, we did not observe clear seasonal trade-offs (Fig. 1, Fig. 8).

Although we only evaluated three of the four conceptualized groups of our framework, omitting the evergreen/fiber-storing species (Fig. 1), we expect that differences in carbon fluxes between evergreen and semi-deciduous fiber-storing species to be small because previous analyses indicated little difference in starch storage, mortality, respiration, or growth between these groups (Hererra-Ramirez et al., 2021). We included the expected behavior of this group in our conceptual framework as reference, which was based on previous observations of species belonging to that group (e.g., *Trattinnickia glaziovii*). Our conceptual framework, in conjunction with our results, helps to improve our understanding of the carbon dynamics in mature trees and provides insights into the mechanisms behind

589 starch accumulation and use and its interplay with carbon sources and sinks that may
590 influence plant survival in tropical forests.

591 **4.1. Semi-deciduous and fiber-storing species have seasonal changes in starch**

592 As we expected, leaf habit influences the seasonal fluctuation of starch in the stemwood.
593 Semi-deciduous species showed significant starch seasonality (p=0.001), while the evergreen
594 species we analyzed did not (Fig. 4). Semi-deciduous trees may experience large imbalances
595 between carbon sources and sinks during the dry season due to the high demand for carbon
596 to rebuild the canopy, and therefore show larger seasonal changes in starch mass than
597 evergreen species (Kozlowski, 1992; Hoch et al., 2003; Würth et al., 2005; Richardson et al.,
598 2013; Furze et al., 2018). This is consistent with studies showing strong seasonality of NSC in
599 temperate deciduous species but not in evergreen species (Chapin et al., 1990; Piispanen and
600 Saranpää, 2001; Trumbore et al., 2015; Martínez-Vilalta et al., 2016; Furze et al., 2018). Our
601 results support the idea that semi-deciduous trees are more dependent on NSC storage than
602 evergreen species in seasonally dry tropical forests. Nevertheless, a larger number of species
603 and a longer time series of NSC dynamics should be examined to confirm these patterns.
604 Histological methods provide a rapid and convenient method for quantifying starch storage
605 that can support observations in a large number of species over the longer term.

606 Our results also suggest that the anatomical distribution of starch in the stemwood influences
607 the seasonal dynamics of NSC (Fig. 5, Fig. S4). The fiber-storing species (*D. microcarpa*) had
608 larger seasonal changes in starch mass than the parenchyma-storing species (Fig. S4). This
609 provides some insight into the mechanisms behind carbon dynamics. In fiber-storing species,
610 the high seasonal carbon consumption may be caused by the larger proportion of living cells
611 in the stem, which require more carbon for respiration than the smaller proportion of living
612 cells in parenchyma-storing species (Fig. 7). This high metabolic cost may compete for carbon

613 resources with other carbon sinks, such as radial growth during the dry season, probably
614 leading to seasonal growth and a high reliance on storage to keep cells alive during low
615 photosynthetic periods. However, the presence of living fibers allows trees to use a larger
616 volume of wood to store starch and cover all metabolic needs, which could reduce their
617 vulnerability to carbon starvation. This would likely benefit plant competition/survival and
618 result in low mortality rates (e.g., Table 1 and Fig S7).

619 **4.2. Fiber-storing species have greater plasticity in radial growth, but not in**
620 **respiration**

621 Trees growing in a seasonally dry environment should balance their carbon sources and sinks
622 in order to survive recurrent stress conditions. The fast-growing, parenchyma-storing species
623 *S. guianensis* kept radial growth relatively constant throughout the year, while the slow-
624 growing, fiber-storing species *D. microcarpa* significantly reduced growth during the dry
625 season (Fig. 6). Thus, these trees, with contrasting starch storage traits and respiration
626 requirements, differentially adjust their balance between carbon sources and sinks during
627 seasonally dry conditions (Fig. 1). It is important to note that radial growth is not the only
628 form of growth in trees, and other forms of growth may be differentially adjusted or
629 prioritized. Nevertheless, reducing radial growth rates during periods of low productivity
630 may make trees more tolerant to a wider range of environmental conditions (Rowland et al.,
631 2023).

632 Contrary to the growth patterns described above, wood respiration did not show seasonal
633 changes for any of the species studied during the year of measurement (Fig. 7). A previous
634 study also reported no changes in CO_2 efflux between dry and wet seasons in tropical forest
635 trees (Asao et al., 2015). CO_2 efflux includes not only wood respiration, but also phloem
636 respiration, CO_2 re-fixation, and transport of CO_2 dissolved in sap (Helm et al., 2023).

637 Nevertheless, it has been shown that some trees can regulate stem CO_2 efflux and growth to
638 adapt to specific environmental conditions, such as seasonal changes in precipitation and
639 temperature, thereby releasing resources for other metabolic activities (Teskey et al., 2008;
640 Huang et al., 2019; Sierra et al., 2022). Thus, it is also possible that the 2019 dry period was
641 not strong enough to induce changes in CO_2 efflux, and longer time series of wood respiration
642 are needed to confirm this pattern.

643 Overall, wood respiration was greatest in the fiber-storing species (*D. microcarpa)*, probably
644 because the proportion of living cells in the wood of this species, which includes parenchyma
645 and living fibers, is greater than in parenchyma-storing species (*S. guianensis* and *O.*
646 *leucoxylon*). Therefore, fiber-storing species may have greater carbon requirements to keep
647 all living wood tissue alive, potentially reducing their ability to regulate respiration
648 seasonally. These results suggest that wood anatomical features of wood, such as living fibers,
649 may indicate a large carbon demand for respiration that may compete strongly with other
650 carbon sinks, such as growth, leading these trees to have a stronger regulation of growth
651 rates and a high reliance on storage. Thus, the proportion of living wood biomass may have
652 greater control over wood respiration than environmental conditions.

653 **4.3. Starch is consumed during the peak of the dry and the wet season**

654 Our results show that, for most trees, starch seems to be consumed not only during the peak
655 of the dry season, but also during the peak of the wet season (Fig. 5, Fig S4). This is clear for
656 *D. microcarpa* and *O. leucoxylon* trees, but we did not observe starch consumption during the
657 wet season for *S. guianensis* (Fig. 5, Fig. S4). We hypothesize that trees may recharge the
658 carbon storage pools during the wet season due to favorable growth and less photosynthetic
659 limitation due to more water availability and lower air temperatures (Dietze et al., 2014).
660 Nevertheless, starch consumption during the wet season suggests a negative carbon balance

661 in these trees. There may be several reasons for this: For fiber-storing trees (*D. microcarpa*),
662 it is possible that the carbon demand of wood growth and respiration exceeds the supply of
663 new photoassimilates. In addition, some other carbon sinks, such as reproduction, may also
664 contribute to a greater carbohydrate demand during the wet season (Hartmann and
665 Trumbore, 2016, Fig. S3). For instance, both *D. microcarpa* and *S. guianensis* produced flowers
666 and fruits during the wet season (Fig. 1, Fig. S3), which may represent a large demand on
667 carbon reserves (Hartmann and Trumbore, 2016; Blumstein et al., 2022). Alternatively, the
668 wet season presents its own challenges that put pressure on available NSC. During the rainy
669 season, blowdowns, storms, and lightning can cause physical damage to trees, which, along
670 with increased herbivory or fungal infections, may increase the risk of individual damage or
671 even mortality (Zuleta et al., 2022, Aleixo et al., 2019). Rebuilding lost tissue during the wet
672 season or building defensive compounds could represent a large demand on NSC (Huang et
673 al., 2021). Thus, trees that have not replenished their NSC reserves and repaired damage
674 during the transition months between the wet and dry seasons may be more vulnerable and
675 susceptible to die when facing stress (Anderegg et al., 2013; Arellano et al., 2019; Aleixo et al.,
676 2019).

677 **4.4. Storage-growth trade-offs occur in fiber-storing species during the wet season**

678 Seasonal patterns in starch mass showed us when trees consumed and accumulated stem
679 NSC. Our results indicate a trade-off between starch consumption/accumulation and growth
680 only during the wet season for the fiber-storing species *D. microcarpa*. For the parenchyma-
681 storing species (*O. leucoxylon* and *S. guianensis*) a storage-growth trade-off was only observed
682 when lagged correlations were considered (Fig. 8), probably reflecting the use of reserves for
683 other metabolic needs, such as reproduction, that are also important for species survival (Fig.
684 S3, Blumstein et al., 2022, Hartmann and Trumbore 2016). Nevertheless, it is important to

clarify that these storage-growth trade-offs may change when other forms of growth are considered. At the whole tree level, the inclusion of other starch storage tissues, such as phloem (Rosell et al., 2021) or roots (Hillman et al., 2021) may provide further insight into these trade-offs.

Identifying trade-offs between C sinks with field measurements is challenging (Blumstein et al., 2022). Here, we show that annual estimates of starch mass and radial stem growth may mask the seasonal trade-offs between these two variables (Fig. S5). This may be influenced by the fact that a single time point measurement of starch mass integrates past fluctuations in plant carbon balance and therefore may not reflect the actual current growing conditions of trees. Also, trade-offs may be influenced by variations in carbon supply. Individuals with higher carbon acquisition may have more leverage to invest more in both growth and storage than individuals with lower carbon acquisition (Blumstein et al., 2022), as may have been the case for our parenchyma-storing species. These two parenchyma-storing species grew faster than the fiber-storing species, and the correlation between annual growth and starch mass was positive for both species during the dry season (August 2019) for *S. guianensis* (Fig. S5e) and during the transition months from wet to dry season (May 2019) for *O. leucoxylon* (Fig. S5j). For more conservative species, such as the fiber-storing species, a weak trade-off trend between starch mass and annual growth was still observed during the wet season (Fig. S5d). Our results suggest that these trade-offs may not be reflected in the annual carbon balance, but only on a seasonal basis. Therefore, evaluating seasonal changes in starch mass (rather than mean storage mass per year or maximum starch storage per year) in relation to seasonal growth may better inform us about when and under what conditions such trade-offs occur, avoiding the influence of some confounding factors when annual averages are used.

Evidence for growth-storage trade-offs is increasing in the literature and has been linked to individual survival (Wright et al., 2004; Poorter and Kitajima, 2007; O'Brien et al., 2014, 2015; Klein and Hoch, 2015; D'Andrea et al., 2019, 2020). Studies comparing highly conservative species and highly competitive species in surviving stressful environmental conditions are needed to further understand how variation in storage-growth trade-offs are maintained across space and time. Our results are a good indication that highly conservative, slow-growing, and high-storage species, such as fiber-storing species (e.g., *D. microcarpa*), may have stronger trade-offs between starch storage and growth, indicating greater plasticity in their sink activity, and/or higher prioritization of storage than parenchyma-storing species. Life history traits such as low growth and low mortality rate are associated with highly conservative species and are a good proxy for tree longevity (Wright et al., 2004; Herrera-Ramírez et al., 2021; Piovesan and Biondi, 2021). Mortality was also lower for the fiber-storing species compared to the parenchyma-storing species evaluated here, not only at background levels in the forest, but also when the forest experienced annual fires (Fig. S7). Therefore, we would expect that as stressors intensify, highly conservative trees, such as fiber-storing species, would have higher survival rates and would become more competitive in seasonally dry forests. Future work should focus on understanding how these species with contrasting anatomical distributions of starch in the stemwood are distributed in forests, and how their different storage-growth trade-offs affect productivity and species survival in tropical forests under climate change.

5. Acknowledgments

We want to thank the Max Planck Society, the Friedrich-Schiller University and the German Research Foundation (SI 1953/2-1) for the founding of this project. Also, we received funding from the EU, through the German Bundesanstalt für Landwirtschaft und Ernährung FKZ:

2816ERA03W (to S. T.); the Brazilian council for Scientific and Technological Development - CNPq (PELD/CNPq No. 441703/2016-0; No. 441940/2020-0; UNIVERSAL No. 430149/2018-2); and DH and ST acknowledge the support from the Balzan foundation.

6. Author contributions

DH-R, CAS, HH, CR, ST, and JM, conceived the idea, conceptualized the hypothesis, and planned the data collection and the experiments. DH, LM-S and DS collected and analyzed data. DH and IK performed sample analysis and quantification. DH-R wrote the manuscript. DH-R, HH, CR, ST, JM, LM-S, PB, DS, HJ, IK, and CAS contributed significantly to the writing of the manuscript and gave important and critical input. All authors revised the manuscript.

7. Data accessibility statement

The data and scripts for calculation and statistical analysis presented here are available in the open GitHub repository “”

8. References

Adams, H. D., Zeppel, M. J. B., Anderegg, W. R. L., Hartmann, H., Landhäusser, S. M., Tissue, D. T., et al. (2017). A multi-species synthesis of physiological mechanisms in drought-induced tree mortality. *Nature Ecology & Evolution* 1, 1285–1291. doi:10.1038/s41559-017-0248-x.

Aleixo, I., Norris, D., Hemerik, L., Barbosa, A., Prata, E., Costa, F., et al. (2019). Amazonian rainforest tree mortality driven by climate and functional traits. *Nature Climate Change* 9, 384–388. doi:10.1038/s41558-019-0458-0.

Anderegg, W. R. L., Berry, J. A., Smith, D. D., Sperry, J. S., Anderegg, L. D. L., and Field, C. B. (2012). The roles of hydraulic and carbon stress in a widespread climate-induced forest die-off. *Proceedings of the National Academy of Sciences* 109, 233–237. doi:10.1073/pnas.1107891109.

Anderegg, W. R. L., Kane, J. M., and Anderegg, L. D. L. (2013). Consequences of widespread tree mortality triggered by drought and temperature stress. *Nature Climate Change* 3, 30–36. doi:10.1038/nclimate1635.

Arellano, G., Medina, N. G., Tan, S., Mohamad, M., and Davies, S. J. (2019). Crown damage and the mortality of tropical trees. *New Phytologist* 221, 169–179. doi:https://doi.org/10.1111/nph.15381.

761 Arx, G. von, Arzac, A., Fonti, P., Frank, D., Zweifel, R., Rigling, A., et al. (2017). Responses of
762 sapwood ray parenchyma and non-structural carbohydrates of pinus sylvestris to drought
763 and long-term irrigation. *Functional Ecology* 31, 1371–1382. doi:10.1111/1365-2435.12860.

764 Asao, S., Bedoya-Arrieta, R., and Ryan, M. G. (2015). Variation in foliar respiration and wood
765 CO_2 efflux rates among species and canopy layers in a wet tropical forest. *Tree Physiology* 35,
766 148–159. doi:10.1093/treephys/tpu107.

767 Barbaroux, C., and Bréda, N. (2002). Contrasting distribution and seasonal dynamics of
768 carbohydrate reserves in stem wood of adult ring-porous sessile oak and diffuse-porous
769 beech trees. *Tree Physiology* 22, 1201–1210. doi:10.1093/treephys/22.17.1201.

770 Blumstein, M., Sala, A., Weston, D. J., Holbrook, N. M., and Hopkins, R. (2022). Plant
771 carbohydrate storage: Intra- and inter-specific trade-offs reveal a major life history trait. *New*
772 *Phytologist* 235, 2211–2222. doi:https://doi.org/10.1111/nph.18213.

773 Canty, A., Ripley, B. D. (2022). *boot: Bootstrap R (S-Plus) Functions*. R package version
774 1.3-28.1.

775 Carlquist, S. (2013). Fibre dimorphism: Cell type diversification as an evolutionary strategy in
776 angiosperm woods. *Botanical Journal of the Linnean Society* 174, 44–67.
777 doi:10.1111/boj.12107.

778 Chapin, F. S., Schulze, E., and Mooney, H. A. (1990). The ecology and economics of storage in
779 plants. *Annual Review of Ecology and Systematics* 21, 423–447.
780 doi:10.1146/annurev.es.21.110190.002231.

781 Davison, A.C., and Hinkley, D. V. (1997). Bootstrap methods and their application, Chapter5.
782 Cambridge University Press.

783 Dietze, M. C., Sala, A., Carbone, M. S., Czimczik, C. I., Mantooth, J. A., Richardson, A. D., et al.
784 (2014). Nonstructural carbon in woody plants. *Annual Review of Plant Biology* 65, 667–687.
785 doi:10.1146/annurev-arplant-050213-040054.

786 D'Andrea, E., Rezaie, N., Battistelli, A., Gavrichkova, O., Kuhlmann, I., Matteucci, G., et al.
787 (2019). Winter's bite: Beech trees survive complete defoliation due to spring late-frost
788 damage by mobilizing old c reserves. *New Phytologist* 224, 625–631.
789 doi:https://doi.org/10.1111/nph.16047.

790 D'Andrea, E., Rezaie, N., Prislan, P., Gričar, J., Collalti, A., Muhr, J., et al. (2020). Frost and
791 drought: Effects of extreme weather events on stem carbon dynamics in a mediterranean
792 beech forest. *Plant, Cell & Environment* 43, 2365–2379.
793 doi:https://doi.org/10.1111/pce.13858.

794 Fox, J. (2015). Applied regression analysis and generalized linear models (3rd ed.). Sage
795 Publications.

796 Fournier, L. A., 1974. Un método cuantitativo para la medición de características fenológicas
797 en árboles. Turrialba 24(4):422-423.

798 Furze, M. E., Huggett, B. A., Chamberlain, C. J., Wieringa, M. M., Aubrecht, D. M., Carbone, M. S.,
799 et al. (2020). Seasonal fluctuation of nonstructural carbohydrates reveals the metabolic

availability of stemwood reserves in temperate trees with contrasting wood anatomy. *Tree Physiology* 40, 1355–1365. doi:10.1093/treephys/tpaa080.

Furze, M. E., Trumbore, S., and Hartmann, H. (2018). Detours on the phloem sugar highway: Stem carbon storage and remobilization. *Current Opinion in Plant Biology* 43, 89–95. doi:https://doi.org/10.1016/j.pbi.2018.02.005.

Galiano, L., Timofeeva, G., Saurer, M., Siegwolf, R., Martínez-Vilalta, J., Hommel, R., et al. (2017). The fate of recently fixed carbon after drought release: Towards unravelling c storage regulation in tilia platyphyllos and pinus sylvestris. *Plant, Cell & Environment* 40, 1711–1724. doi:https://doi.org/10.1111/pce.12972.

Hartmann, H., and Trumbore, S. (2016). Understanding the roles of nonstructural carbohydrates in forest trees from what we can measure to what we want to know. *New Phytologist* 211, 386–403. doi:10.1111/nph.13955.

Hartmann, H., McDowell, N. G., and Trumbore, S. (2015). Allocation to carbon storage pools in Norway spruce saplings under drought and low CO_2. *Tree Physiology* 35, 243–252. doi:10.1093/treephys/tpv019.

Hartmann, H., Ziegler, W., and Trumbore, S. (2013). Lethal drought leads to reduction in nonstructural carbohydrates in norway spruce tree roots but not in the canopy. *Functional Ecology* 27, 413–427. doi:https://doi.org/10.1111/1365-2435.12046.

Helm, J., Salomón, R.L., Hilman, B., Muhr, J., Knohl, A., Steppe, K. et al. (2023). Differences between tree stem CO2 efflux and O2 influx rates cannot be explained by internal CO2 transport or storage in large beech trees. *Plant, Cell & Environment*, 1– 14. https://doi.org/10.1111/pce.14614

Herrera-Ramírez, D., Sierra, C. A., Römermann, C., Muhr, J., Trumbore, S., Silvério, D., et al. (2021). Starch and lipid storage strategies in tropical trees relate to growth and mortality. *New Phytologist* 230, 139–154. doi:https://doi.org/10.1111/nph.17239.

Hilman, B., Muhr, J., Helm, J., Kuhlmann, I., Schulze, E.-D., & Trumbore, S. (2021). The size and the age of the metabolically active carbon in tree roots. *Plant, Cell & Environment* 44(8), 2522– 2535. https://doi.org/10.1111/pce.14124

Hoch, G., Richter, A., and Körner, C. (2003). Non-structural carbon compounds in temperate forest trees. *Plant, Cell & Environment* 26, 1067–1081. doi:10.1046/j.0016-8025.2003.01032.x.

Holm, S. (1979). A Simple Sequentially Rejective Multiple Test Procedure. *Scandinavian Journal of Statistics*, *6*(2), 65–70. http://www.jstor.org/stable/4615733

Hollander, M., Wolfe, D. A., and Chicken, E. (2013). Nonparametric statistical methods (3rd ed.). John Wiley & Sons.

Huang, J., Hammerbacher, A., Gershenzon, J., Dam, N. M. van, Sala, A., McDowell, N. G., et al. (2021). Storage of carbon reserves in spruce trees is prioritized over growth in the face of carbon limitation. *Proceedings of the National Academy of Sciences* 118, e2023297118. doi:10.1073/pnas.2023297118.

839 Huang, J., Rücker, A., Schmidt, A., Gleixner, G., Gershenzon, J., Trumbore, S., et al. (2020).
840 Production of constitutive and induced secondary metabolites is coordinated with growth
841 and storage in Norway spruce saplings. *Tree Physiology* 40, 928-942.
842 doi:https://doi.org/10.1093/treephys/tpaa040.

843 Huang, J., Hammerbacher, A., Weinhold, A., Reichelt, M., Gleixner, G., Behrendt, T., et al.
844 (2019). Eyes on the future – evidence for trade-offs between growth, storage and defense in
845 norway spruce. *New Phytologist* 222, 144–158. doi:https://doi.org/10.1111/nph.15522.

846 Klein, T., and Hoch, G. (2015). Tree carbon allocation dynamics determined using a carbon
847 mass balance approach. *New Phytologist* 205, 147–159. doi:10.1111/nph.12993.

848 Kozlowski, T. T. (1992). Carbohydrate sources and sinks in woody plants. *The Botanical*
849 *Review* 58, 107–222. doi:10.1007/BF02858600.

850 Körner, C. (2003). Carbon limitation in trees. *Journal of Ecology* 91, 4–17.
851 doi:https://doi.org/10.1046/j.1365-2745.2003.00742.x.

852 Landhäusser, S. M., Chow, P. S., Dickman, L. T., Furze, M. E., Kuhlman, I., Schmid, S., et al.
853 (2018). Standardized protocols and procedures can precisely and accurately quantify non-
854 structural carbohydrates. *Tree Physiology* 38, 1764–1778. doi:10.1093/treephys/tpy118.

855 Martínez-Vilalta, J. (2014). Carbon storage in trees: pathogens have their say. *Tree Physiology*
856 34, 215–217. doi:10.1093/treephys/tpu010.

857 Martínez-Vilalta, J., Sala, A., Asensio, D., Galiano, L., Hoch, G., Palacio, S., et al. (2016). Dynamics
858 of non-structural carbohydrates in terrestrial plants: A global synthesis. *Ecological*
859 *Monographs* 86, 495–516. doi:https://doi.org/10.1002/ecm.1231.

860 Meir, P., Mencuccini, M., and Coughlin, S. I. (2020). Respiration in wood: Integrating across
861 tissues, functions and scales. *New Phytologist* 225, 1824–1827.
862 doi:https://doi.org/10.1111/nph.16354.

863 Michelot, A., Simard, S., Rathgeber, C., Dufrêne, E., and Damesin, C. (2012). Comparing the
864 intra-annual wood formation of three European species (Fagus sylvatica, Quercus petraea
865 and Pinus sylvestris) as related to leaf phenology and non-structural carbohydrate dynamics.
866 *Tree Physiology* 32, 1033–1045. doi:10.1093/treephys/tps052.

867 Muhr, J., Trumbore, S., Higuchi, N. and Kunert, N. (2018), Living on borrowed time –
868 Amazonian trees use decade-old storage carbon to survive for months after complete stem
869 girdling. *New Phytologist*, 220: 111-120. https://doi.org/10.1111/nph.15302

870 Newell, E. A., Mulkey, S. S., and Wright, J. S. (2002). Seasonal patterns of carbohydrate storage
871 in four tropical tree species. *Oecologia* 131, 333–342. doi:10.1007/s00442-002-0888-6.

872 O'Brien, M. J., Burslem, D. F. R. P., Caduff, A., Tay, J., and Hector, A. (2015). Contrasting
873 nonstructural carbohydrate dynamics of tropical tree seedlings under water deficit and
874 variability. *New Phytologist* 205, 1083–1094. doi:https://doi.org/10.1111/nph.13134.

875 O'Brien, M. J., Leuzinger, S., Philipson, C. D., Tay, J., and Hector, A. (2014). Drought survival of
876 tropical tree seedlings enhanced by non-structural carbohydrate levels. *Nature Climate*
877 *Change* 4, 710 EP. Available at: http://dx.doi.org/10.1038/nclimate2281.

878 O'Brien, M. J., Valtat, A., Abiven, S., Studer, M. S., Ong, R., and Schmid, B. (2020). The role of
879 soluble sugars during drought in tropical tree seedlings with contrasting tolerances. *Journal*
880 *of Plant Ecology* 13, 389–397. doi:10.1093/jpe/rtaa017.

881 Palacio, S., Hoch, G., Sala, A., Körner, C., and Millard, P. (2014). Does carbon storage limit tree
882 growth? *New Phytologist* 201, 1096–1100. doi:10.1111/nph.12602.

883 Peltier, D. M., Nguyen, P., Ebert, C., Koch, G. W., Schuur, E. A., Ogle, K., (2023). Moisture stress
884 limits radial mixing of non-structural carbohydrates in sapwood of trembling aspen, *Tree*
885 *Physiology*, tpad083, https://doi.org/10.1093/treephys/tpad083

886 Piispanen, R., and Saranpää, P. (2001). Variation of non-structural carbohydrates in silver
887 birch (betula pendula roth) wood. *Trees* 15, 444–451. doi:10.1007/s004680100125.

888 Piovesan, G., and Biondi, F. (2021). On tree longevity. *New Phytologist* 231, 1318–1337.
889 doi:https://doi.org/10.1111/nph.17148.

890 Piper, F. I., and Paula, S. (2020). The role of nonstructural carbohydrates storage in forest
891 resilience under climate change. *Current Forestry Reports* 6, 1–13. doi:10.1007/s40725-019-
892 00109-z.

893 Piper, F. I., Gundale, M. J., and Fajardo, A. (2015). Extreme defoliation reduces tree growth but
894 not C and N storage in a winter-deciduous species. *Annals of Botany* 115, 1093–1103.
895 doi:10.1093/aob/mcv038.

896 Plavcová, L., Hoch, G., Morris, H., Ghiasi, S., and Jansen, S. (2016). The amount of parenchyma
897 and living fibers affects storage of nonstructural carbohydrates in young stems and roots of
898 temperate trees. *American Journal of Botany* 103, 603–612. doi:10.3732/ajb.1500489.

899 Poorter, L., and Kitajima, K. (2007). Carbohydrate storage and light requirements of tropical
900 moist and dry forest tree species. *Ecology* 88, 1000–1011. doi:https://doi.org/10.1890/06-
901 0984.

902 R Core Team (2023). _R: A Language and Environment for Statistical Computing_. R
903 Foundation for Statistical Computing, Vienna, Austria. <https://www.R-project.org/>.

904

905 Resco de Dios, V., and Gessler, A. (2021). Sink and source co-limitation in the response of
906 stored non-structural carbohydrates to an intense but short drought. *Trees* 35, 1751–1754.
907 doi:10.1007/s00468-021-02116-9.

908 Richardson, A. D., Carbone, M. S., Keenan, T. F., Czimczik, C. I., Hollinger, D. Y., Murakami, P., et
909 al. (2013). Seasonal dynamics and age of stemwood nonstructural carbohydrates in
910 temperate forest trees. *New Phytologist* 197, 850–861. doi:10.1111/nph.12042.

911 Rosell, J. A., Piper, F. I., Jiménez-Vera, C., Vergílio, P. C., Marcati, C. R., et al. (2021). Inner bark
912 as a crucial tissue for non-structural carbohydrate storage across three tropical woody plant
913 communities. *Plant, Cell & Environment* 44, 156– 170. doi:10.1111/pce.13903

914 Rowland, L., Ramírez-Valiente, J. A., Hartley, I. P. and Mencuccini, M. (2023), How woody
915 plants adjust above- and below-ground traits in response to sustained drought. *New*
916 *Phytologist*, 239: 1173-1189. https://doi.org/10.1111/nph.19000

Sala, A., Woodruff, D. R., and Meinzer, F. C. (2012). Carbon dynamics in trees: Feast or famine? *Tree Physiology* 32, 764–775. doi:10.1093/treephys/tpr143.

Salleo, S., Lo Gullo, M. A., Trifilò, P., and Nardini, A. (2004). New evidence for a role of vessel-associated cells and phloem in the rapid xylem refilling of cavitated stems of laurus nobilis l. *Plant, Cell & Environment* 27, 1065–1076. doi:10.1111/j.1365-3040.2004.01211.x.

Schneider, C. A., Rasband, W. S., and Eliceiri, K. W. (2012). NIH image to imagej: 25 years of image analysis. *Nature Methods* 9, 671–675. doi:10.1038/nmeth.2089.

Sevanto, and M., Sanna, Dickman, L Turin, Pangle, Robert E., and Pockman, W. T. (2014). How do trees die? A test of the hydraulic failure and carbon starvation hypotheses. *Plant, Cell & Environment* 37, 153–161. doi:10.1111/pce.12141.

Sierra, C. A., Ceballos-Núñez, V., Hartmann, H., Herrera-Ramírez, D., and Metzler, H. (2022). Ideas and perspectives: Allocation of carbon from net primary production in models is inconsistent with observations of the age of respired carbon. *Biogeosciences* 19, 3727–3738. doi:10.5194/bg-19-3727-2022.

Teskey, R. O., Saveyn, A., Steppe, K., and McGuire, M. A. (2008). Origin, fate and significance of CO_2 in tree stems. *New Phytologist* 177, 17–32. doi:https://doi.org/10.1111/j.1469-8137.2007.02286.x.

The GIMP Development Team. (2019). *GIMP*. Retrieved from https://www.gimp.org

Trumbore, S., Czimczik, C. I., Sierra, C. A., Muhr, J., and Xu, X. (2015). Non-structural carbon dynamics and allocation relate to growth rate and leaf habit in California oaks. *Tree Physiology* 35, 1206–1222. doi:10.1093/treephys/tpv097.

Wiley, E., and Helliker, B. (2012). A re-evaluation of carbon storage in trees lends greater support for carbon limitation to growth. *New Phytologist* 195, 285–289. doi:https://doi.org/10.1111/j.1469-8137.2012.04180.x.

Wiley, E., Casper, B. B., and Helliker, B. R. (2017). Recovery following defoliation involves shifts in allocation that favour storage and reproduction over radial growth in black oak. *Journal of Ecology* 105, 412–424. doi:https://doi.org/10.1111/1365-2745.12672.

Wright, I. J., Reich, P. B., Westoby, M., Ackerly, D. D., Baruch, Z., Bongers, F., et al. (2004). The worldwide leaf economics spectrum. *Nature* 428, 821–827. doi:10.1038/nature02403.

Würth, M. K. R., Peláez-Riedl, S., Wright, S. J., and Körner, C. (2005). Non-structural carbohydrate pools in a tropical forest. *Oecologia* 143, 11–24. doi:10.1007/s00442-004-1773-2.

Zuleta, D., Arellano, G., Muller-Landau, H. C., McMahon, S. M., Aguilar, S., Bunyavejchewin, S., et al. (2022). Individual tree damage dominates mortality risk factors across six tropical forests. *New Phytologist* 233, 705–721. doi:https://doi.org/10.1111/nph.17832.

Zweifel, R., Haeni, M., Buchmann, N., and Eugster, W. (2016). Are trees able to grow in periods of stem shrinkage? *New Phytologist* 211, 839–849. doi:https://doi.org/10.1111/nph.13995.

954 Zweifel, R., Zimmermann, L., Zeugin, F., and Newbery, D. M. (2006). Intra-annual radial
955 growth and water relations of trees: implications towards a growth mechanism. *Journal of*
956 *Experimental Botany* 57, 1445–1459. doi:10.1093/jxb/erj125.

957

958 **9. Tables**

959 Table 1: Species names and traits: wood storage strategy, growth rates, mortality rates,

960 phenology, and the sampling dates.

Species name	Growth rate (cm/year)	Mortality rate (%/year)	Storage strategy	Leaf phenology (~% of leaf loss)
Ocotea leucoxylon (Sw.) Laness	0.295	5.7	Parenchyma	Evergreen (~30)
Sacoglottis guianensis Benth.	0.72	5.0	Parenchyma	Semi-deciduous (~45)
Dacryodes microcarpa Cuart.	0.078	1.6	Fiber	Semi-deciduous (~60)

961

962

963

964